arXiv:1406.2711v2 [cond-mat.str-el] 1 Dec 2014

Nematic and spin-charge orders driven by hole-doping a charge-transfer insulator

Mark H. Fischer[1,2], Si Wu[3], Michael Lawler[1], Arun Paramekanti[3,4], Eun-Ah Kim[1]

[1] Department of Physics, Cornell University, Ithaca, New York 14853, USA
[2] The Weizmann Institute of Science, Rehovot 7610001, Israel
[3] Department of Physics, University of Toronto, Toronto, Ontario M5S 1A7, Canada
[4] Canadian Institute for Advanced Research, Toronto, Ontario M5G 1Z8, Canada

Abstract. Recent experimental discoveries have brought a diverse set of broken symmetry states to the center stage of research on cuprate superconductors. Here, we focus on a thematic understanding of the diverse phenomenology by exploring a strong-coupling mechanism of symmetry breaking driven by frustration of antiferromagnetic order. We achieve this through a variational study of a three-band model of the CuO_2 plane with Kondo-type exchange couplings between doped oxygen holes and classical copper spins. Two main findings from this strong-coupling multi-band perspective are 1) that the symmetry hierarchy of spin stripe, charge stripe, intra-unit-cell nematic order and isotropic phases are all accessible microscopically within the model, 2) many symmetry-breaking patterns compete with energy differences within a few meV per Cu atom to produce a rich phase diagram. These results indicate that the diverse phenomenology of broken-symmetry states in hole-doped antiferromagnetic charge-transfer insulators may indeed arise from hole-doped frustration of antiferromagnetism.

1. Introduction

Translational-symmetry breaking in hole-doped La-based nickelates and cuprates in the form of static spin and charge stripes has been well established for almost two decades [1–4]. However, until recently, the ubiquity of such phenomena had not been clear. The recent surge of experimental discoveries reporting spin or charge order in all families of hole-doped cuprates [5–21] and even in some Fe-based superconductors [22] has brought the diverse phenomenology of broken-symmetry states to the forefront of study of high T_c superconductors. In particular there is extensive indication that $\mathbf{Q} = 0$ intra-unit-cell (IUC) orders [11, 15, 16, 18, 19] and (short-ranged) $\mathbf{Q} \neq 0$ modulations [5, 6, 8–10, 12] coexist. In this new landscape of ubiquitous and diverse forms of broken-symmetry reports, an emerging central question is whether the diverse set of phenomena share a common origin or if each phenomenon should be studied on its own.

Closely linked to the question of whether a thematic understanding of the observed phenomena is attainable is a theoretical question of whether to take the weak-coupling Fermi-surface instability perspective or to take the strong-coupling perspective. From

a Fermi-surface instability perspective, the simultaneous occurrence of multiple orders requires fine tuning as one usually finds a single dominant instability in one ordering channel. For instance, it was shown that antiferromagnetic exchange interactions [23] or short-range repulsive interactions [24] can drive an instability towards density modulation along an incommensurate vector $\mathbf{Q} = (Q_0, Q_0)$ with a dominantly d-form factor. Although a $\mathbf{Q} = 0$ order with the d-form factor will be equivalent to IUC nematic order observed in various experiments [15, 16], a modulation at finite $\mathbf{Q}$ will not show net IUC nematicity, just as antiferromagnets have no net magnetization. However, from a strong coupling perspective that focuses on the influence of *local* antiferromagnetic correlations, multiple orders could naturally intertwine.

While it is to be expected on symmetry grounds that a nematic order [25] will be more robust and may coexist with disordered stripes [26], microscopic studies so far have focused on either finite $\mathbf{Q}$ ordering of spin and charge stripe phenomena [27–32] or $\mathbf{Q} = 0$ IUC nematic phenomena [14,17,33–38]. Moreover, since simple Hartree-Fock mean-field theories incorrectly predict insulating period-8 stripes [27–30], the present theoretical understanding of the experimentally observed metallic period-4 charge stripes at doping $x = 1/8$ [2] is dependent upon elaborate variational numerical studies [31, 39–43] or the scenario of Coulomb-frustrated phase separation [44]. Our goal is to capture a wide range of spin and charge ordered states, including those experimentally observed, in a simple microscopic model that retains the strong-coupling aspect of hole-doping that enables holes to frustrate antiferromagnetic order in the "parent compound". A successful demonstration of close energetic competition between diverse outcomes from the same root of local anti-ferromagnetic correlations would be an important step towards thematic understanding of the observed diverse phenomena.

Although it is well known that motion of doped holes will frustrate the antiferromagnetic background of the cuprate "parent compounds" [45], much of the work on this issue has largely focused on the one-band Hubbard model as a minimal framework to discuss this physics. Nevertheless, a host of experimental observations on cuprate superconductors (e.g., electron-hole doping asymmetry of the phase diagram and unusual broken-symmetry phases with spin and charge order [5–21] at low hole doping) strongly call for a description which explicitly retains the oxygen orbitals. Such multi-orbital models of the CuO_2 plane, like the Emery model [46], are, however, even less amenable to a theoretical treatment than the one-band Hubbard model.

In this paper, we consider a simplified model which ignores the charge fluctuation on the transition metal sites and treat the spins on those sites as classical local moments that interact with doped itinerant holes living on the oxygen sites through a Kondo type coupling (see Figure 1). This is a tractable three-orbital model that retains the spatial separation between the local moments on Cu and the doped holes that predominantly go into oxygen sites. We consider several plausible spin-order patterns and exactly solve for the many-hole eigenstates associated with the spin-order patterns. This way we can access not only the lowest energy spin-hole configuration, but investigate how magnetism drives charge physics in the cuprates, study the energetic competition between a wide

range of spin and charge ordered states, and gain insight into the interplay between spin and intra-unit-cell nematic orders [15].

Before proceeding to the model Hamiltonian and our analysis, we clarify the nature of the charge and spin order parameters that will characterize the various phases we consider in the paper. We define the IUC nematic order parameter, which measures the inequivalence of the hole density between the x- and y-oxygen sites within the CuO_2 unit cell as

$$\eta \equiv \frac{n_x - n_y}{n_x + n_y}, \tag{1}$$

where n_x and n_y are the expectation value of the hole density at the x- and y- oxygen sites respectively. The charge stripe order parameter is also extracted from the hole density as the Fourier component at a finite $\mathbf{Q} \neq \mathbf{0}$, $n(\mathbf{Q}) \equiv \sum_j e^{i\mathbf{Q}\cdot x_j}\langle c_j^\dagger c_j\rangle$. Finally, spin stripe and spiral order parameters of interest are Fourier components of the spin density at a finite $\mathbf{Q}$, $\langle\vec{S}(\mathbf{Q})\rangle$ where $\vec{S}$ is either co-linear (stripe) or co-planar (spiral). From a symmetry perspective, any state with non-zero $n(\mathbf{Q})$ or $\langle\vec{S}(\mathbf{Q})\rangle$ for one $\mathbf{Q}$ (i.e., uni-directional modulation), breaks spatial rotational symmetry as well as translational symmetry. Such a phase is referred to as electronic smectic [25]. When the modulation vector lies along the Cu-O bond direction, there will be a symmetry allowed coupling between the modulation order parameters and the IUC nematic order parameter η resulting in $\eta \neq 0$ in the presence of long range modulational order,i.e., $n(\mathbf{Q}) \neq 0$ or $\langle\vec{S}(\mathbf{Q})\rangle \neq 0$. Hence, a discussion of the IUC nematic order parameter for our ansatz modulational states may appear inconsequential. However, when heterogeneity and thermal fluctuations cause the experimentally observed modulational orders to be short-ranged, a microsopic understanding of how the IUC nematic order parameter η can locally relate to spin and charge modulations is crucial in making contact between theory and experiments [47]. Hence, we believe it is important to study the microscopic behavior of both order parameters even for the case of ideal long-ranged modulations.

The rest of the paper is organized as follows. In section 2 we introduce and motivate the model as well as the choice of some parameters. In section 3 we discuss the choice of spin-ordering configuration ansätze. In section 4 we discuss the charge-ordered states we obtain associated with each spin-ordering configuration. In section 5 we discuss the energy differences between different ansätze and the phase diagram. In section 6 the effect of a nearest-neighbor oxygen-oxygen interaction is analyzed. Finally, we conclude with a summary and discussion in section 7.

2. Model

In this paper we restrict our attention to the Hilbert space with singly occupied Cu $d_{x^2-y^2}$ orbitals represented as local moments that interact antiferromagnetically. The doped holes will be assumed to go into the oxygen p_x or p_y orbitals [46]. These holes couple to the local moments on Cu sites through both (spin-dependent) hopping between O sites mediated by Cu sites and spin-spin interactions. Treating the moments on the

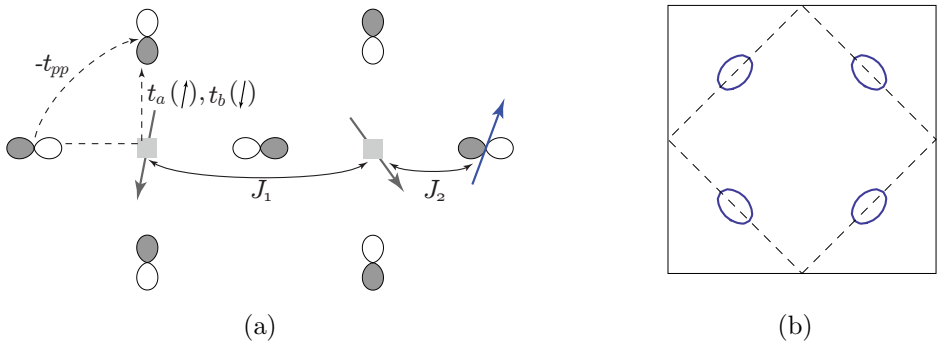


Figure 1. (a) Unit cell of the CuO_2 plane showing a localized copper spin with mobile spinful holes on the surrounding oxygen p_x and p_y orbitals. Also indicated are the direct (t_{pp}) and the via-Cu hopping processes with the spin of the hole antiparallel (t_a) and parallel (t_b) to the copper spin, as well as exchange interaction parameters that define our model. (b) The hole-like Fermi surfaces in the antiferromagnetic Néel ordered state at $x \approx 5\%$ doping of our model Hamiltonian for parameter values $t_a = 0.3$, $t_b = 0.275$, and $t_{pp} = 0.15$ (see Appendix A). This choice of parameters leads to a minimum at the nodal $(\pm\pi/2, \pm\pi/2)$ points in agreement with ARPES experiments on the extremely underdoped cuprate [48].

Cu sites classically, we arrive at a model Hamiltonian

$$\mathcal{H} = \frac{t_a - t_b}{2} \sum_{\langle IiI' \rangle, s} \hat{p}^\dagger_{Is} \hat{p}_{I's} + (t_a + t_b) \sum_{\langle IiI' \rangle, s, s'} \vec{S}_i \cdot (\hat{p}^\dagger_{Is} \vec{\sigma}_{ss'} \hat{p}_{I's'}) - t_{pp} \sum_{\langle II' \rangle, s} \hat{p}^\dagger_{Is} \hat{p}_{I's} + J_1 \sum_{\langle i,j \rangle} \vec{S}_i \cdot \vec{S}_j + J_2 \sum_{\langle i,I \rangle, s, s'} \vec{S}_i \cdot (\hat{p}^\dagger_{Is} \vec{\sigma}_{ss'} \hat{p}_{Is'}), \quad (2)$$

where $\hat{p}_{Is}$ are the oxygen hole annihilation operators at oxygen site I with spin s, $\vec{S}_i$ is a classical spin vector at Cu-site i with $|\vec{S}_i| = 1/2$, and $\vec{\sigma}$ are the Pauli matrices. The first two terms represent two hopping processes through the Cu sites, the t_a (t_b) process with hole spin anti-parallel (parallel) to $\vec{S}_i$. These hopping processes amount to nearest- and next-nearest-neighbor hopping on the lattice of oxygen sites. Note that the second term in equation (2) hence introduces coupling between the motion of the holes on O-sites and the spin on the Cu sites. The third term represents direct hopping between O-sites, which amounts to nearest-neighbor hopping on the lattice of oxygen sites. The last two terms represent exchange coupling between Cu spins (the J_1 term) and between a Cu spin and the hole spin on a neighboring O site (the J_2 term).

The model Hamiltonian of equation (2) is a simplified form of a perturbative expansion in Cu-O hopping t_{pd} (to order t^4_{pd}) in the large Coulomb interaction limit of the Emery model Hamiltonian for the cuprates [46]: $\mathcal{H} = \mathcal{H}_0 + \mathcal{H}'$ with

$$\mathcal{H}_0 = t_{pd} \sum_{\langle i,I \rangle, s} (\hat{d}^\dagger_{is} \hat{p}_{Is} + \text{h.c.}) - t_{pp} \sum_{\langle I,I' \rangle, s} \hat{p}^\dagger_{Is} \hat{p}_{I's} - \mu \sum_{i,s} \hat{n}^d_{is} - (\mu - \Delta) \sum_{I,s} \hat{n}^p_{Is} \quad (3)$$

and

$$\mathcal{H}' = U_d \sum_i \hat{n}^d_{i\uparrow} \hat{n}^d_{i\downarrow} + U_p \sum_I \hat{n}^p_{I\uparrow} \hat{n}^p_{I\downarrow} + V_{pd} \sum_{\langle i,I \rangle, s, s'} \hat{n}^d_{is} \hat{n}^p_{Is'} + V_{pp} \sum_{\langle I,I' \rangle, s, s'} \hat{n}^p_{Is} \hat{n}^p_{I's'}. \quad (4)$$

However, the actual model obtained through such perturbative expansion is still highly non-trivial as it does not allow double occupancy at oxygen sites and the spins on Cu-sites should be quantum mechanical spins. Frenkel et al [49] studied the exact quantum ground state of such a model in the presence of a single hole in a small cluster. Despite the reduction of the Hilbert space due to the constraint of singly occupied Cu $d_{x^2-y^2}$ orbitals, the largest cluster they could study was a 4×4 Cu-O cluster which would be too small to see the observed stripe phenomena. Such studies have been extended to larger clusters [50] with the aim of understanding spin polaron formation in a 3-band model. However, this exact diagonalization study is restricted to 1-hole and 2-hole states in the undoped insulator and thus cannot address doping dependent competing orders. By treating the local moments on Cu sites to be classical and relaxing the no-double-occupancy constraint on oxygen sites, we arrive at the more tractable model Hamiltonian of equation (2).

Our simple model has several features. Firstly, it is a solvable model that retains much of the microscopic details and non-trivial interactions of under-doped cuprates. The solvability of the model allows us to study a wide variety of states including incommensurate orderings. Secondly, we expect similar effective models are applicable to other doped strongly-correlated charge-transfer insulators such as the nickelates. In particular, a classical approximation of the local moment on the transition-metal ion is likely to be a better approximation in Ni given its larger moment. Finally, through spatial separation between spins and holes, the model offers a rich playground for strong-coupling-driven spin and charge orders co-existing with intra-unit-cell nematic order.

Earlier consideration of the strong-coupling limit of the Emery model by Kivelson et al. [51] focused on the limit of vanishing inter-oxygen site hopping. In that limit, the dynamics is strictly one-dimensional and hence the ground state is a nematic phase. Three key differences between the limit considered in Ref. [51] and the limit captured by our model equation (2) are that 1) we have taken U_d to be so strong to the extent that we suppressed the charge fluctuation in the Cu sites, 2) we consider inter-oxygen hopping to be comparable to exchange interactions, and 3) we take the Cu-O exchange interaction into account. As a result, the charge dynamics in our model is strictly two dimensional. However we make the approximation of leaving out U_p and V_{pp} which yields an exactly solvable model for the hole motion on a system size that can exhibit translational symmetry breaking. This approximation may not affect the conclusions qualitatively in the limit of dilute hole density.

Although the model Hamiltonian has quite a few parameters, many of them are constrained by experiments. We use a Cu-Cu exchange interaction $J_1 \sim 125$meV, close to the value estimated for La_2CuO_4 from neutron scattering studies of the spin-wave dispersion [52]. In order to constrain hopping strengths, we examine the dispersion of a single hole doped in an ordered Néel antiferromagnet. We can diagonalize the hole Hamiltonian assuming an out of plane spin moment on Cu atoms in an antiferromagnetic arrangement, *i.e.* $S_i^z = \frac{1}{2}(-1)^{i_x+i_y}$, and obtain four dispersing bands (see Appendix A). The resulting lowest dispersion can be compared to the ARPES measurements on

extremely underdoped cuprates [48]. Although the ARPES energy distribution curves are broad, we can infer the following energy scales from the peak positions. The binding energy at $(\pi/2, \pi/2)$ is lower than that at $(\pi, 0)$ by about 300meV [48], which corresponds to $2t_{pp}$; this fixes $t_{pp} = 150$meV. Shen et al. [48] also found that the spectral peaks disperse by about 1.4eV going from the Γ-point to $(\pi/2, \pi/2)$. In our model, this energy difference is just $4t_b + 2t_{pp}$; this fixes $t_b = 275$meV. Cluster diagonalization calculations in Ref. [49, 53] indicate that t_a is the same sign as t_b, with $|t_b - t_a| \ll t_a + t_b$. We therefore examine a range of values $t_b/2 < t_a < 3t_b/2$. The above choice of hopping parameters yields a Fermi surface consisting of hole-pockets centered at $(\pm\pi/2, \pm\pi/2)$ for the $\hat{p}_{Is}$ holes (see Fig. 1(b)), consistent with the energy minimum of a single hole in the Néel ordered antiferromagnet being centered at $(\pm\pi/2, \pm\pi/2)$. We expect the antiferromagnetic Cu-O exchange interaction J_2, which is only present at finite doping, to be stronger than the Cu-Cu exchange J_1. Hence we explore a range of $J_1 < J_2 < 3J_1$. We note that our values for the parameters in the effective Hamiltonian for doped holes differ slightly from those used in previous work [49, 53, 54] - the values we use should be viewed as effective couplings given our assumption of a classical copper spin. They also place the regime of interest in the strong coupling limit, since $t_a + t_b$ and J_2 are much greater than the free fermion bandwidth set by $|t_a - t_b| \sim t_{pp}$ and motivate the use of a variational approach as discussed in the next and following sections.

3. Ansätze for spin-order configurations

The key mechanism by which the model Hamiltonian of equation (2) drives spin and charge order at finite doping is the frustration of antiferromagnetic order in the parent compound (i.e., zero doping). The undoped cuprate and nickelate insulators are ordered antiferromagnets, possessing long-range Néel order in planes which are stacked along the c axis. The planar Néel order has a wavevector (π, π) and is a collinear state with $\vec{S}_i = S\hat{n}(-1)^{i_x+i_y}$ with $\hat{n}$ being a unit vector. Doped oxygen holes frustrate the antiferromagnetic alignment of Cu moments driven by the Cu-Cu exchange J_1 through a strong antiferromagnetic Cu-O exchange interaction J_2. Thus, doped holes promote a ferromagnetic arrangement of the two neighboring local Cu-moments and drive spatial symmetry breaking in the spin configuration. Interestingly, such frustration is not expected in the electron-doped cuprates, where doped electrons go onto Cu sites. This naturally explains why the Néel order is present to much higher doping in electron doped cuprates whereas the hole-doped cuprates exhibit various broken-symmetry states.

While ultimately the model equation (2) can be exactly solved by combining Monte Carlo simulation of the spin problem with the exact diagonalization of the fermion problem, we here consider two classes of spin-order configurations and solve the fermion problem within each class. This approach offers us an understanding of the parameter-space landscape. Moreover, although our understanding is limited to the set of ansatz spin patterns we consider, this approach has the advantage over the explicit solution in that it allows us to compare energetics of different candidate states. The two classes we

consider are coplanar spin spirals and collinear spin stripes with different wave vector $\mathbf{Q}$. As there is much literature on both of these candidate states we defer in-depth discussion to review articles (see e.g., [55, 56]). Rather, we discuss aspects of these states that are directly relevant to our study and the rationale for their consideration below.

(i) **Coplanar spin spirals:** While a doped hole promotes ferromagnetic correlations of the local moments in its vicinity, the spins far from the hole maintain their Néel correlations. Hence, in the absence of magnetic anisotropy a coplanar spiral state may be expected as a solution that interpolates between the Néel order and ferromagnetism when holes are doped into a quantum antiferromagnet as it has been argued in Ref. [57]. However, spiral states are accompanied by translationally invariant charge distribution and they are unstable against magnetic anisotropy as well as phase separation. Further, susceptibility studies [58] in spin-ordered cuprates are consistent with collinear order. However, the smoking-gun polarized neutron scattering experiment has not been performed to date and local spiral distortions of the spin background may be an appropriate picture in the insulating regime at low doping [59].

Below, we pick the spiral to lie in the $S_x - S_y$ plane, setting $\vec{S}_i = S(\cos \mathbf{Q}\cdot\mathbf{r}_i, \sin \mathbf{Q}\cdot\mathbf{r}_i, 0)$, and consider different propagation wavevectors $\mathbf{Q}$ running parallel to the Cu-O bonds (labelled **Psp1**, **Psp2**) or along the diagonal direction (**Dsp**), see Fig. 2, and compute their physical properties and energies. We show that within a three-orbital picture, the spin spirals with a wavevector parallel to the Cu-O bonds are naturally accompanied by a translationally invariant oxygen hole density, but with *charge nematic order* on the oxygen sites as has been observed in STS experiments [15]. This opens up a possibility of disordered spiral leaving the discrete and robust nematic order as the only observable effect. Similar ideas have been perviously considered in the context of frustrated magnets [60].

(ii) **Stripes:** Two theoretical approaches discussed stripes prior to their experimental observations. The first approach was that of Hartree-Fock mean-field theory [27–30] which predicted insulating (fully filled) period-8 charge stripes at $x = 1/8$ doping. The other approach was built on the observation that phase separation should be expected in t-J models for $J \gg t$, where 'slow' doped holes cluster together to avoid disrupting the Néel order of the local moments [61]. This led to the proposal that stripe orders could emerge as periodic density modulations due to frustration of such phase separation by long-range Coulomb interactions [44]. Following the experimental observation of metallic period-4 charge stripe at $x = 1/8$ doping in La-based cuprates [2], theoretical efforts focused on going beyond Hartree-Fock mean-field theory to obtain the observed metallic stripe [31, 39–43]. A particularly convincing case was made by a density matrix renormalization group study by White and Scalapino [31] which not only obtained the observed metallic stripe ground states at $x = 1/8$ but also demonstrated that anti-phase domain walls between collinear antiferromagnetic domains attract charge stripes. This issue of charge stripe periodicity (period-4 and metallic v.s. period-8 and insulating) bears particular importance in the discussion of the role of charge stripes in superconductivity [32]. However, most previous efforts at going

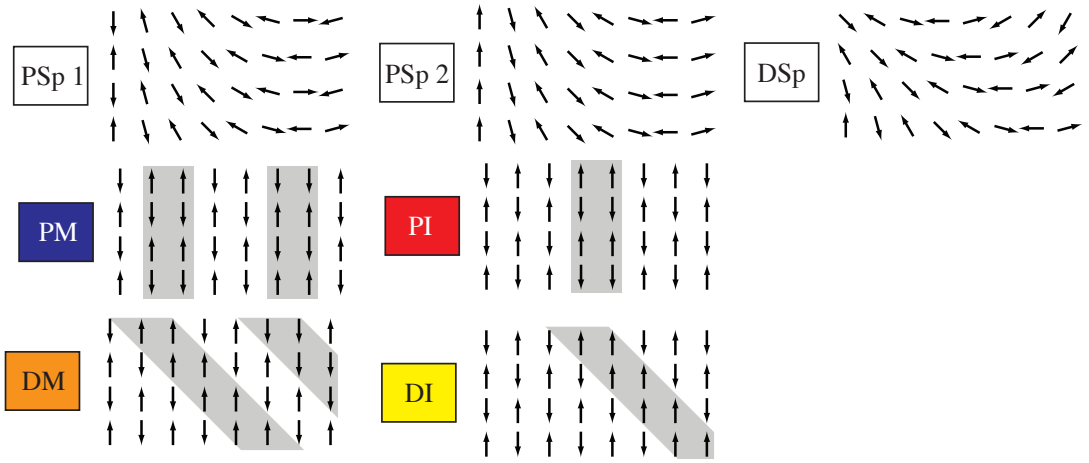


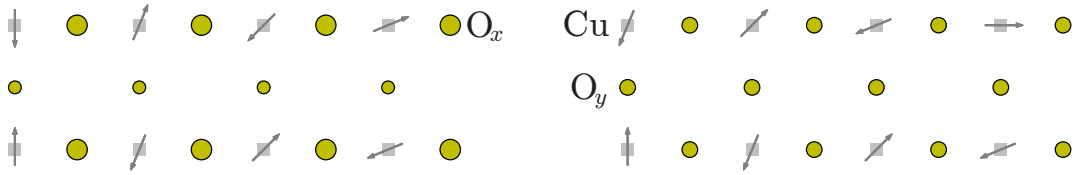
Figure 2. Catelog of Ansätze used in our variational calculations in the form of the classical spin configurations of local moments on Cu atoms. The gray areas in the stripe patterns denote anti-phase domain walls between antiferromagnetic domains.

beyond Hartree-Fock mean-field theory and incorporating strong-coupling physics relied on sophisticated numerics. The spatial separation of Cu-moment and doped holes in our model allows us to investigate the complex spin-charge interplay in the strong-coupling regime in a transparent manner. In our model, spin-antiphase domain walls can form upon hole-doping to relieve the frustration between the AFM order favored by Cu-Cu antiferromagnetic superexchange interactions and the ferromagnetic order favored by an antiferromagnetic Cu-O exchange.

We model the spin stripes as antiphase domain walls in the collinear antiferromagnet and consider several different uni-directional domain-wall configurations depending on the direction of periodicity as well as the period. Note that these spin stripes will be bond-centered by construction. We consider parallel stripes with wave vectors $\mathbf{Q}$ along the Cu-O bond directions as well as diagonal stripes with $\mathbf{Q}$ at 45^o angle with respect to Cu-O bond direction. At fixed hole density of $x = 1/8$, different periods determine whether the stripe can support metallic transport along the stripe: period-4 parallel charge stripe (labeled **PM**, see Fig 2) will be half-filled and metallic while period-8 parallel charge stripe (labeled **PI**, see Fig 2) will be fully-filled and insulating. Similarly, one can consider metallic (labeled **DM**, see Fig 2) and insulating (labeled **DI**, see Fig 2) diagonal stripes.

4. Charge orders associated with different spin-order ansätze

For each spin-order candidate, we diagonalize the (quadratic) hole Hamiltonian and use the resulting lowest-energy many-hole wave function and the spin configuration to evaluate the total energy for the spin-charge-ordered state. The total energy for a given spin configuration $\{\vec{S}\}$ at a given doping $x = n/N$, with N the number of Cu-O unit



(a) Psp1 (b) Dsp

Figure 3. A representative oxygen-hole charge distribution $n_{x,y}$ are shown through yellow circles for (a) a parallel spiral Psp1 and (b) a diagonal spiral with $x = 1/8$. The size of yellow circles represent the magnitude of charge density at the site. The parallel spiral shows non-zero nematic order $\eta \neq 0$.

cells, is given by

$$E(\{\vec{S}\})/N = \frac{1}{N}\sum_{l<n}\xi_l(\{\vec{S}\}) + \frac{1}{N}E^{\mathrm{Cu-Cu}}(\{\vec{S}\}), \tag{5}$$

where $\xi_l(\{\vec{S}\})$ are the (energy-ordered) eigenvalues of the Hamiltonian (2) for the given configuration $\{\vec{S}\}$. In equation (5) the last term is the interaction energy due to Cu-Cu exchange (the J_1 term in equation (2)).

For the spiral configurations given by $\vec{S}_i = S(\cos \mathbf{Q}\cdot\mathbf{r}_i, \sin \mathbf{Q}\cdot\mathbf{r}_i, 0)$ we take advantage of a closed form of the Hamiltonian equation (2) in momentum space (See Appendix A) to find the wave vector $\mathbf{Q}$ that minimizes the energy for each spiral. Fig. 3 shows the lowest-energy charge distribution for a parallel spiral (Fig. 3(a)) and a diagonal spiral (Fig. 3(b)) spin configurations. Though it is well known that spiral order of spins would not be accompanied by any charge modulation, Fig. 3(a) shows that parallel-spiral tendency drives IUC nematic charge order (for $t_a = 200$meV and $J_2 = 200$meV, we find $\eta \approx 5\%$ for the Cu-spin configuration in Figure 3). Note that even when the spiral order of the spins is disordered due to thermal or quantum fluctuations, the discrete symmetry breaking of IUC nematic in the charge sector can be more robust.

For the collinear stripe configurations, we consider a lattice of 32×32 unit cells (2048 oxygen sites) and diagonalize the quadratic Hamiltonian of the holes only living on the oxygen site, equation (2). The resulting charge-order patterns for different trial spin configurations (see Fig. 4) clearly show that the holes are attracted to the anti-phase domain walls in the spin configurations driven by the Cu-O exchange-coupling J_2. The kinetic terms broaden the hole distribution and favor the metallic charge stripe. It is remarkable that our simple model can readily access the spin and charge striped ground-state configuration reminiscent of those obtained in density matrix renormalization group studies of the 1/8-doped t-J model [31]. Moreover, as this model incorporates the mostly-oxygen character of doped holes, the charge stripes centered at the anti-phase domain wall of the antiferromagnetic background are naturally coupled to IUC nematic. The parallel stripe configurations obtained in Fig. 4 clearly demonstrate a coupling between the (Ising) IUC nematic order and the stripe-ordering wave vector.

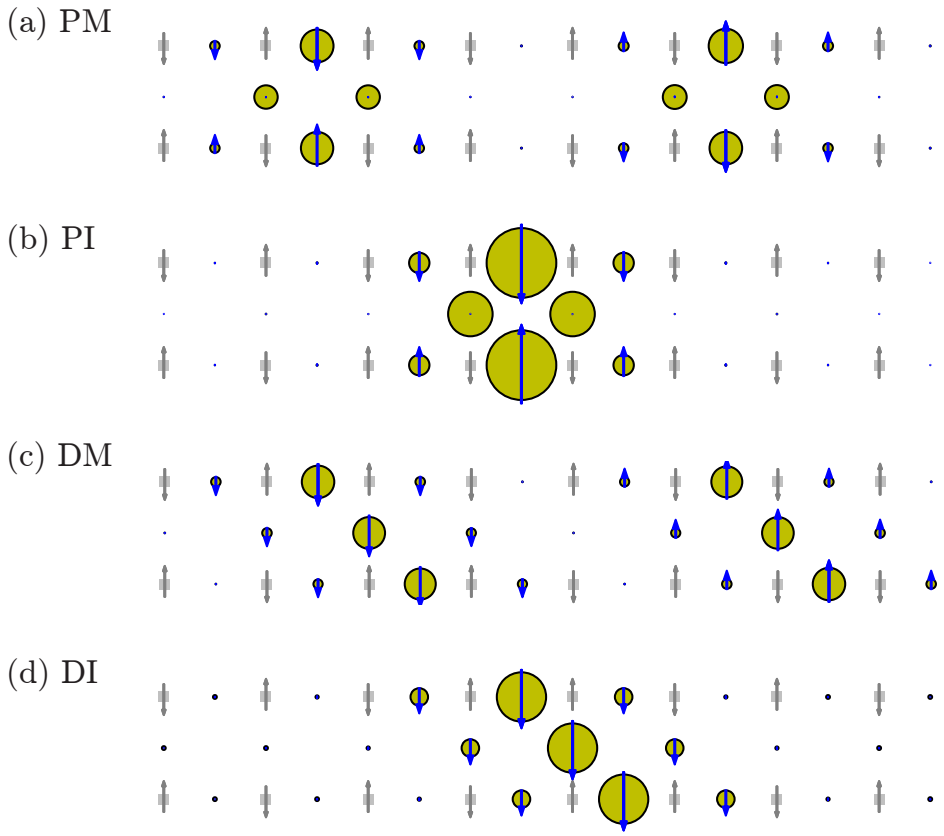


Figure 4. Charge distribution (depicted by the size of the yellow circles) and spin polarization (length of blue arrows) of oxygen holes for (a) metallic and (b) insulating parallel stripes, as well as (c) metallic and (d) insulating diagonal stripes for $t_a = 200$meV and $J_2 = 200$meV. Note that the length of the (spin) arrow on the oxygen site is scaled by a factor of 5 as compared to the Cu sites.

In the sense of Ginzburg-Landau theory of order parameters, Fig. 4 demonstrates a coupling between the Ising nematic order parameter and the difference in amplitude of the charge-density wave (CDW) order parameters for CDW's propagating along the two Cu-O bond directions [62] at a microscopic level. The charge distribution we obtain for trial spin configurations in Figs. 3 and 4 makes it clear that any spin order with modulation vector along the Cu-O bond direction will be accompanied by IUC nematic irrespective of charge stripe order. ‡ The remaining question is which of these candidate states is lowest in energy and what are the energy differences between competing states.

‡ On symmetry grounds, any unidirectional spin order along Cu-O bond direction breaks the point group symmetry and hence it can, in principle, couple to nematic order parameter; what is new here is an explicit microscopic realization of such a coupling.

5. Phase diagram

While our variational study is limited by the choice of states we consider, it has the advantage of allowing the energetic comparison between different candidate states over Hartree-Fock or variational Monte Carlo studies. Surprisingly, we find the entire collection of states we consider to show close energetic competition. For the most part of the parameter space we consider (varying hopping through Cu t_a and Cu-O exchange J_2) different states differ in energy only by a few meV. The close energetic competition is clear in Figure 5 which shows energy differences as a function of t_a at fixed $J_2 = 170$meV. Such close competition indicates small perturbations to our model Hamiltonian such as spin-orbit coupling or lattice anisotropies could change the phase diagram significantly.

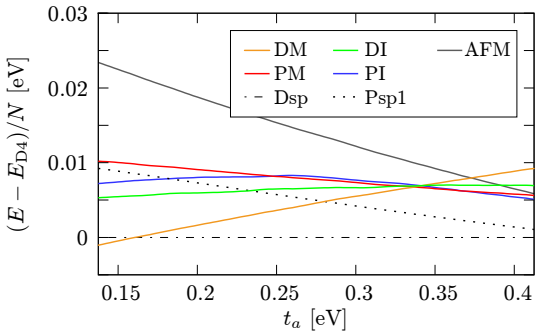


Figure 5. The energy difference of all the states in our Ansatz catelog (see Fig. 2) compared to the diagonal spiral state (Dsp) as a function of t_a for $J_2 = 170$meV (dashed line in the phase diagram in Figure 6(b)). Shown are the antiferromagnetic (AFM), the parallel spiral (Psp1), the diagonal spiral (Dsp), as well as the diagonal metallic stripe (DM), diagonal insulating stripe (DI) parallel metallic stripe (PM), and parallel insulating stripe (PI). Notice the parallel orders are preferred for larger t_a.

It is well known that incorporating quantum fluctuations of spins strongly favors collinear order over coplanar or non-coplanar states [63, 64], Similarly, spin anisotropy due to weak spin-orbit coupling could also hinder coplanar spirals. We therefore present two phase diagrams here: a phase diagram that includes co-planar spiral and a phase diagram that only concerns collinear orders. Figure 6(a) shows the phase diagram that allows for co-planar spiral as a function of hopping through Cu-sites t_a and the Cu-O exchange J_2. We have limited the plotting range of J_2 to be a reasonable range of 100meV $< J_2 <$ 300meV. Figure 6(a) shows that the lowest-energy configuration with the parameters motivated from cuprates is dominated by diagonal orders such as diagonal spiral or diagonal metallic stripe. In the limit of large J_2 (not shown), parallel spiral with IUC nematic appears before Cu spins align ferromagnetically. Figure 6(b) shows the phase diagram restricted to collinear orders. Notably metallic diagonal and parallel stripe orders appear in a substantial region of the phase diagram. The close competition between diagonal stripe order and parallel stripe order is remarkable in light of the experimentally known transition from diagonal to parallel stripe upon doping [65]. The parallel metallic charge stripe order (PM) at $x = 1/8$ is consistent with observations

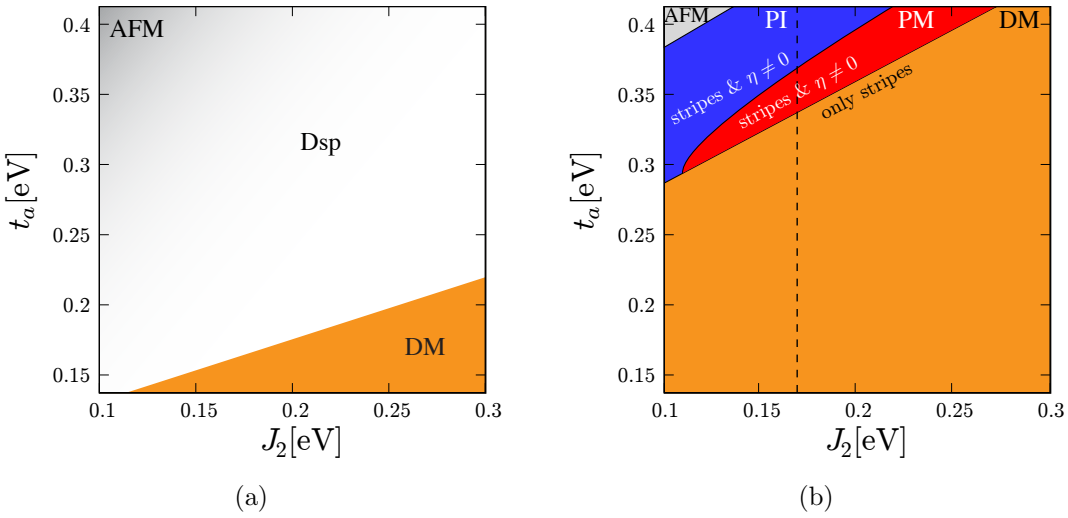


Figure 6. (a) Full phase diagram at $x = 1/8$ with all phases allowed as a function of the Cu-O spin-spin interaction J_2 and the hopping t_a. (b) the phase diagram if we only allow collinear order for the Cu spins. The parameters used are $t_b = 275$meV, $J_1 = 125$meV and $t_{pp} = 150$meV. Parallel stripes show non-zero IUC nematicity $\eta \neq 0$ (see Eq. 1).

in La-based compounds [65, 66] as well as those in Bi-based compounds [5, 6, 15, 62].

The microscopic tie between spin-ordering patterns and charge-ordering patterns resulting from our simple model depicted in Figs. 3 and 4 hints at a microscopic mechanism of charge order without spin order at finite temperature [67]. The spin orders under consideration require breaking of spin rotational symmetry as well as spatial translation and point-group symmetries while charge orders only break spatial symmetries. While the driving force for charge order in our model is the frustration of antiferromagnetic order upon holes entering oxygen sites, fluctuations in spin space will suppress spin order. It has been shown in the context of Fe-based superconductors [68] that spin fluctuations $\langle|\vec{S}_{\mathbf{Q}}|^2\rangle \neq 0$ in the absence of spin order ($\langle\vec{S}_{\mathbf{Q}}\rangle = 0$) can drive nematicity. Similarly, since the cuprates are quasi-2D systems, it is quite plausible that thermal fluctuations may prevent spin order in the stripe state, while $\langle|\vec{S}_{\mathbf{Q}}|^2\rangle \neq 0$ may still leave the charge order visible. This can be easily seen by the fact that the charge stripe and IUC nematic in the parallel stripe phases in Fig. 4 as well as IUC nematic in the parallel spiral phase in Fig. 3 are insensitive to the spin-orientation, so (thermal) averaging over the global spin orientation will leave these orders unaffected. Hence, charge order in Fig. 3 can onset without detectable spin order or with a lower temperature transition into a state with coexisting spin order. This would amount to a microscopic realization of a so-called "charge-driven transition" in the Landau theory study Ref. [69]. Experimental observations of charge and/or spin order in cuprate families broadly show such preferential visibility of charge order [5, 6, 8–10, 15, 62, 65, 66].

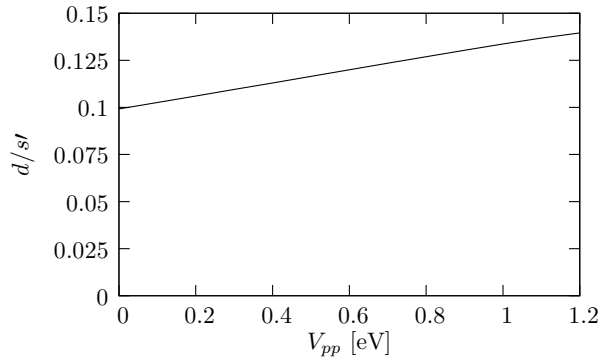


Figure 7. The effect of V_{pp} on the relative importance between s'-form factor and d-form factor components of charge-density waves for $t_a = 350$meV and $J_2 = 170$meV for the PM state.

6. Effects of inter-oxygen repulsion V_{pp}

As IUC nematic naturally accompanies all modulations along the Cu-O bond directions within our model, it is natural to ask what would be the effect of the inter-oxygen repulsion V_{pp} that was found to drive IUC nematic [38, 51]. Recently Bulut et al. [24] extended the mean-field study by two of us [38] to include the charge-density wave instability as well as IUC nematic instability. They found the d-form factor component $\psi^d(\mathbf{r})$, defined on oxygen sites using the notation of Ref. [23] via

$$\rho(\mathbf{r}) = \mathrm{Re}\left[\left(f^s(\mathbf{r})\psi^s(\mathbf{r}) + f^{s'}(\mathbf{r})\psi^{s'}(\mathbf{r}) + f^d(\mathbf{r})\psi^d(\mathbf{r})\right)e^{i\mathbf{Q}\cdot\mathbf{r}}\right], \tag{6}$$

where $f^s(\mathbf{r})$ ($f^{s'}(\mathbf{r})$) is zero (one) on copper sites and one (zero) on oxygen sites and $f^d(\mathbf{r})$ is zero on copper sites, one on x oriented oxygen sites and minus one on y-oriented oxygen sites, to dominate the density wave instability along the Brillouin zone diagonal. While different form-factor components of density waves are not symmetry distinct, experimental observation of the d-form factor [5, 70] hints at the importance of microscopic interactions promoting an anti-phase relation between the two oxygen sites [70].

As charge fluctuations on Cu-sites have been projected out in our model ($\psi^s(\mathbf{r}) = 0$), charge stripes found in our model consist only of s'- and d-form factor components. In order to study the effect of V_{pp} on the charge configurations associated with candidate spin configurations, we treat the V_{pp} term at the level of self-consistent Hartree approximation. As experiments observe $\mathbf{Q} = \mathbf{0}$ IUC nematic simultaneously with short-ranged d-form factor density waves [70] we focused the study to the parameter space where a Cu-O bond-direction charge stripe is present in the absence of V_{pp}.

On symmetry grounds, $\psi^{s'}(\mathbf{r})$, $\psi^d(\mathbf{r})$ and IUC nematic order parameter can form a cubic coupling within Landau theory. Hence, we generically expect both s'- and d-form factor components to be present given the robust IUC nematicity coexisting with charge stripes in our charge-ordering patterns. For $t_a = 350$meV, $J_2 = 170$meV, figure 7 shows the resulting ratio of the d- and s'- form factor components. While the density waves we obtained for the PM configuration have predominantly s'-form factor, Fig. 7

clearly shows that V_{pp} promotes a d-form factor for the charge stripe along the Cu-O bond direction with the wave vector consistent with the experimental observations.

7. Discussion

To summarize, we considered a three-orbital model for underdoped cuprates, which incorporates strong-coupling physics through singly occupied Cu-sites hosting local moments and reflects the charge-transfer energy through constraining holes to live on the oxygen sites. We took a variational approach for the spin configurations and solved for many-hole states exactly for each configuration at $x = 1/8$ doping. We found that the balance between the Cu-Cu exchange interaction, the kinetic energy of holes and the Kondo type coupling between the Cu spins and the spin of the holes conspire to a rich phase diagram featuring several experimentally observed phases. What is more interesting is the close energetic competition between the candidate states such as co-planar spirals, diagonal stripes and parallel stripes with different wave lengths. Within this model, any parallel order including co-planar spiral orders exhibit non-zero IUC nematic order parameter, providing a microscopic mechanism for robustness of a IUC nematic. The mechanism for nematicity considered in this paper differs from the weak-coupling fermi-surface instability driven by a so-called F_2 interaction [35, 36] or inter-oxygen repulsion V_{pp} [38] in that we focus on the strong local antiferromagnetic correlations between singly occupied Cu sites as the driving force for nematicity.

Though we studied the parameter space constrained by various experiments on the cuprates, our model can be applied to other transition metal oxides like the doped nickelates which exhibit similar spin-charge ordered states as cuprates [1]. In the nickelates, a local moment at Ni sites may arise from the effect of strong Hund's coupling between two electrons (or two holes) in the two e_g orbitals, leading to an orbital singlet and a spin-triplet $S = 1$ state. This spin-triplet nature of the local moment suppresses hopping through Ni sites which renders the system insulating at all doping ($x < 0.9$) without ever exhibiting superconductivity. Antiferromagnetism is more robust in Nickelates and extends to hole concentration of $n_h = x + 2\delta \sim 0.2$ before it is replaced by fully filled diagonal stripe order [1]. Indeed, we find the diagonal insulating stripe as most favored co-linear order in the limit $t_a \ll J_1 < J_2$.

Recently, several model studies investigating the Fermi-surface instability towards formation of charge-density waves [23, 24, 71–74] have found charge-density waves with predominantly d-form factor. Some theories focused on the "hot spot" regions of the Fermi surface, where antiferromagnetic scattering will be especially strong near the antiferromagnetic quantum critical point [23, 71], while others considered one-band models with d-form factor interactions [72, 73] or a three-band model [24]. Though the prominence of the d-form factor component in the density waves appear compatible with experiments [5, 70], these models universally obtained charge-density waves with the wave vector along the Brillouin zone diagonal, i.e., diagonal stripes. This direction and the magnitude of the wave vector is at odds with experimental findings of parallel

stripes. More recently, Atkinson et al [74] showed that the wave vector found in Ref. [24] can be rotated to lie in the Cu-O bond direction by assuming large staggered moments which reconstruct the Fermi surface. However, experimentally it is known that antiferromagnetic fluctuations at (π, π) are replaced by incommensurate magnetic peaks at temperatures well above the charge ordering temperature in inelastic neutron scattering at low energies [65,75]. Moreover, nematic ordering which appears to be most robust in experiments, only appear as sub-dominant instability in these Fermi-surface instability studies [23, 24, 71–74].

In this paper, we took a strong-coupling approach of projecting out charge fluctuation at the Cu-sites yet dealing with an exactly solvable model by ignoring quantum fluctuations of spins at the Cu-sites. In this approach, we found $\mathbf{Q} = 0$ IUC nematic to naturally coexist with any modulation along the Cu-O direction be it co-planar spiral or collinear spin stripes. This is in contrast with weak-coupling Fermi-surface-instability approaches finding competition between $\mathbf{Q} = 0$ order and $\mathbf{Q} \neq 0$ density waves. Also, we find various experimentally observed charge-ordered states (diagonal insulating stripe, diagonal metallic stripe, parallel metallic stripe) to dominate at different parts of the physically-motivated parameter space exhibiting a close competition. The understanding of the parameter space of our model we gained from the present variational approach can guide us in the attempt for a more explicit exact solution of the model combining Monte Carlo simulations with exact diagonalization.

Before closing, we turn to the implications of our results for the experimentally observed broken symmetry states in different cuprate families (summarized in Refs. [47, 76, 77]). Although d-wave superconductivity is robust in all the cuprate families, the recent detection of charge order in $YBa_2Cu_3O_{6+x}$ reveals material specific differences regarding the issue of competing broken symmetry states. The La-214 family exhibits spin order at wave vector $\mathbf{Q}_s = \mathbf{Q}_c/2$ where $\mathbf{Q}_s$ and $\mathbf{Q}_c$ are spin and charge modulation wave vectors respectively, while $YBa_2Cu_3O_{6+x}$ with $x > 0.8$ does not appear to have static spin order. BSCCO and La-214 families appear to have period-4 charge order at 1/8 doping, while $YBa_2Cu_3O_{6+x}$ has incommensurate order with a period close to $3a_0$. In BSCCO and La-214, the charge order wavevector grows with increasing hole doping while it appears to shrink in $YBa_2Cu_3O_{6+x}$. Nevertheless, all cuprate families indicate incommensurate spin correlations (static or dynamic) whose wavevector grows with doping. Can such a diverse phenomena of competing orders be captured within a unified microscopic framework?

Regarding the issue of spin order, our variational study shows that within our strong coupling mechanism, a long-ranged spin stripe order with wave vector $\mathbf{Q}_s$ leads to a charge stripe at wave vector $2\mathbf{Q}_s$. On the other hand, the present study cannot address whether a charge stripe driven by local antiferromagnetic correlations would necessarily require spin order; indeed, broken lattice symmetries might be more stable against quantum and thermal fluctuations, and thus survive even if long-range spin order itself melts. For instance, it has already been shown that when charge order has a higher

transition temperature, spin order may or may not occur at the level of Landau theory of coupled order parameters [69]. Regarding the issue of the doping dependence of the ordering wave vector, our present study has only focused on one doping of $x = 1/8$. Here we found the period-4 metallic to be the lowest energy state in a part of the parameter space which is consistent with the wave vectors found in La-214 compounds and BSCCO compounds but different from the wave vector found in $YBa_2Cu_3O_{6+x}$ at the same doping. However, what is more significant is the finding that the simple model Hamiltonian of Equation (2) can select lowest energy states with varying wave lengths and properties depending on the microscopic parameters. Specifically, the spin correlations in $YBa_2Cu_3O_{6+x}$ might be more strongly dictated by the Fermi surface of the doped holes, leading to different charge ordering wavevector, which may allow one to reconcile the apparently quite different observed broken symmetries in this family of materials. In conclusion, our results support the view that despite system-specific differences, the various symmetry-breaking phenomena can be driven by same driving force of local magnetic correlations.

Acknowledgements: We thank Erez Berg, W. Buyers, J.C. Seamus Davis, Eduardo Fradkin, Marc-Henri Julien, Steve Kivelson, Kai Sun, John Tranquada for helpful discussions. M.H.F was supported in part by Cornell Center for Materials Research with funding from the NSF MRSEC program (DMR-1120296) and by the Swiss Society of Friends of the Weizmann Institute of Science. E.-A.K was supported by the U.S. Department of Energy, Office of Basic Energy Sciences, Division of Materials Science and Engineering under Award DE-SC0010313. S.W. and A.P. acknowledge funding from NSERC of Canada.

[1] J. M. Tranquada, D. J. Buttrey, V. Sachan, and J. E. Lorenzo. Simultaneous ordering of holes and spins in $La_2NiO_{4.125}$. *Phys. Rev. Lett.*, 73:1003–1006, Aug 1994.

[2] J. M. Tranquada, B. J. Sternlieb, J. D. Axe, Y. Nakamura, and S. Uchida. Evidence for stripe correlations of spins and holes in copper oxide superconductors. *Nature*, 375(6532):561–563, 06 1995.

[3] J. M. Tranquada, J. D. Axe, N. Ichikawa, Y. Nakamura, S. Uchida, and B. Nachumi. Neutron-scattering study of stripe-phase order of holes and spins in $La_{1.48}Nd_{0.4}Sr_{0.12}CuO_4$. *Phys. Rev. B*, 54:7489–7499, Sep 1996.

[4] P. Abbamonte, A. Rusydi, S. Smadici, G. D. Gu, G. A. Sawatzky, and D. L. Feng. Spatially modulated 'mottness' in $La_{2-x}Ba_xCu)_4$. *Nat Phys*, 1(3):155–158, 12 2005.

[5] R. Comin, A. Frano, M. M. Yee, Y. Yoshida, H. Eisaki, E. Schierle, E. Weschke, R. Sutarto, F. He, A. Soumyanarayanan, Yang He, M. Le Tacon, I. S. Elfimov, Jennifer E. Hoffman, G. A. Sawatzky, B. Keimer, and A. Damascelli. Charge order driven by fermi-arc instability in $Bi_2Sr_{2-x}La_xCuO_{6+\delta}$. *Science*, 343(6169):390–392, 2014.

[6] Eduardo H. da Silva Neto, Pegor Aynajian, Alex Frano, Riccardo Comin, Enrico Schierle, Eugen Weschke, András Gyenis, Jinsheng Wen, John Schneeloch, Zhijun Xu, Shimpei Ono, Genda Gu, Mathieu Le Tacon, and Ali Yazdani. Ubiquitous interplay between charge ordering and high-temperature superconductivity in cuprates. *Science*, 343(6169):393–396, 2014.

[7] Arkady Shekhter, B. J. Ramshaw, Ruixing Liang, W. N. Hardy, D. A. Bonn, Fedor F. Balakirev, Ross D. McDonald, Jon B. Betts, Scott C. Riggs, and Albert Migliori. Bounding the pseudogap with a line of phase transitions in $YBa_2Cu_3O_{6+\delta}$. *Nature*, 498(7452):75–77, 06 2013.

[8] E. Blackburn, J. Chang, M. Hücker, A. T. Holmes, N. B. Christensen, Ruixing Liang, D. A. Bonn, W. N. Hardy, U. Rütt, O. Gutowski, M. v. Zimmermann, E. M. Forgan, and S. M. Hayden. X-ray diffraction observations of a charge-density-wave order in superconducting ortho-ii $YBa_2Cu_3\mathbf{O}_{6.54}$ single crystals in zero magnetic field. *Phys. Rev. Lett.*, 110:137004, Mar 2013.

[9] J. Chang, E. Blackburn, A. T. Holmes, N. B. Christensen, J. Larsen, J. Mesot, Ruixing Liang, D. A. Bonn, W. N. Hardy, A. Watenphul, M. v. Zimmermann, E. M. Forgan, and S. M. Hayden. Direct observation of competition between superconductivity and charge density wave order in $YBa_2Cu_3O_{6.67}$. *Nat Phys*, 8(12):871–876, 12 2012.

[10] A. J. Achkar, R. Sutarto, X. Mao, F. He, A. Frano, S. Blanco-Canosa, M. Le Tacon, G. Ghiringhelli, L. Braicovich, M. Minola, M. Moretti Sala, C. Mazzoli, Ruixing Liang, D. A. Bonn, W. N. Hardy, B. Keimer, G. A. Sawatzky, and D. G. Hawthorn. Distinct charge orders in the planes and chains of ortho-iii-ordered $YBa_2Cu_3\mathbf{O}_{6+\delta}$ superconductors identified by resonant elastic x-ray scattering. *Phys. Rev. Lett.*, 109:167001, Oct 2012.

[11] S. De Almeida-Didry, Y. Sidis, V. Balédent, F. Giovannelli, I. Monot-Laffez, and P. Bourges. Evidence for intra-unit-cell magnetic order in $Bi_2Sr_2CaCu_2O_{8+\delta}$. *Phys. Rev. B*, 86:020504, Jul 2012.

[12] G. Ghiringhelli, M. Le Tacon, M. Minola, S. Blanco-Canosa, C. Mazzoli, N. B. Brookes, G. M. De Luca, A. Frano, D. G. Hawthorn, F. He, T. Loew, M. Moretti Sala, D. C. Peets, M. Salluzzo, E. Schierle, R. Sutarto, G. A. Sawatzky, E. Weschke, B. Keimer, and L. Braicovich. Long-range incommensurate charge fluctuations in (Y,Nd)$Ba_2Cu_3O_{6+x}$. *Science*, 337(6096):821–825, 2012.

[13] Tao Wu, Hadrien Mayaffre, Steffen Kramer, Mladen Horvatic, Claude Berthier, W. N. Hardy, Ruixing Liang, D. A. Bonn, and Marc-Henri Julien. Magnetic-field-induced charge-stripe order in the high-temperature superconductor $YBa_2Cu_3O_y$. *Nature*, 477(7363):191–194, 09 2011.

[14] S. Okamoto, D. Sénéchal, M. Civelli, and A.-M. S. Tremblay. Dynamical electronic nematicity from mott physics. *Phys. Rev. B*, 82(18):180511, Nov 2010.

[15] M.J. Lawler, K. Fujita, Lee Jhinwhan, Schmidt A. R., Kohsaka Y, Kim Chum Koo, Hiroshi Eisaki, Uchida S, J. C. Davis, Sethna J.P., and Kim Eun-Ah. Intra-unit-cell electronic nematicity of the high-T_c copper-oxide pseudogap states. *Nature*, 466:347–351, May 2010.

[16] R. Daou, J. Chang, David LeBoeuf, Olivier Cyr-Choiniere, Francis Laliberte, Nicolas Doiron-Leyraud, B. J. Ramshaw, Ruixing Liang, D. A. Bonn, W. N. Hardy, and Louis Taillefer. Broken rotational symmetry in the pseudogap phase of a high-T_c superconductor. *Nature*, 463(7280):519–522, 01 2010.

[17] Emanuel Gull, Olivier Parcollet, Philipp Werner, and Andrew J. Millis. Momentum-sector-selective metal-insulator transition in the eight-site dynamical mean-field approximation to the Hubbard model in two dimensions. *Phys. Rev. B*, 80(24):245102, Dec 2009.

[18] Y. Li, V. Baledent, N. Barisic, Y. Cho, B. Fauque, Y. Sidis, G. Yu, X. Zhao, P. Bourges, and M. Greven. Unusual magnetic order in the pseudogap region of the superconductor $HgBa_2CuO_{4+\delta}$. *Nature*, 455(7211):372–375, 09 2008.

[19] H. A. Mook, Y. Sidis, B. Fauqué, V. Balédent, and P. Bourges. Observation of magnetic order in a superconducting $YBa_2Cu_3O_{6.6}$ single crystal using polarized neutron scattering. *Phys. Rev. B*, 78:020506, Jul 2008.

[20] Jing Xia, Elizabeth Schemm, G. Deutscher, S. A. Kivelson, D. A. Bonn, W. N. Hardy, R. Liang, W. Siemons, G. Koster, M. M. Fejer, and A. Kapitulnik. Polar kerr-effect measurements of the high-temperature $YBa_2Cu_3O_{6+x}$ superconductor: Evidence for broken symmetry near the pseudogap temperature. *Phys. Rev. Lett.*, 100:127002, Mar 2008.

[21] V. Hinkov, D. Haug, B. Fauqué, P. Bourges, Y. Sidis, A. Ivanov, C. Bernhard, C. T. Lin, and B. Keimer. Electronic liquid crystal state in the high-temperature superconductor $YBa_2Cu_3O_{6.45}$. *Science*, 319(5863):597–600, 2008.

[22] S. Kasahara, H. J. Shi, K. Hashimoto, S. Tonegawa, Y. Mizukami, T. Shibauchi, K. Sugimoto, T. Fukuda, T. Terashima, Andriy H. Nevidomskyy, and Y. Matsuda. Electronic nematicity above the structural and superconducting transition in $BaFe_2(As_{1-x}Px)_2$. *Nature*,

486(7403):382–385, 06 2012.

[23] Subir Sachdev and Rolando La Placa. Bond order in two-dimensional metals with antiferromagnetic exchange interactions. *Phys. Rev. Lett.*, 111:027202, Jul 2013.

[24] S. Bulut, W. A. Atkinson, and A. P. Kampf. Spatially modulated electronic nematicity in the three-band model of cuprate superconductors. *Phys. Rev. B*, 88:155132, Oct 2013.

[25] S. A. Kivelson, E. Fradkin, and V. J. Emery. Electronic liquid-crystal phases of a doped mott insulator. *Nature*, 393(6685):550–553, 06 1998.

[26] S.A. Kivelson Laimei Nie, Gilles Tarjus. Quenched disorder and vestigial nematicity in the pseudogap regime of the cuprates. arXiv:1311.5580.

[27] D. Poilblanc and T. M. Rice. Charged solitons in the hartree-fock approximation to the large- U Hubbard model. *Phys. Rev. B*, 39:9749–9752, May 1989.

[28] Kazushige Machida. Magnetism in La_2CuO_4 based compounds. *Physica C: Superconductivity*, 158(1–2):192 – 196, 1989.

[29] H. J. Schulz. Incommensurate antiferromagnetism in the two-dimensional Hubbard model. *Phys. Rev. Lett.*, 64:1445–1448, Mar 1990.

[30] Jan Zaanen and Olle Gunnarsson. Charged magnetic domain lines and the magnetism of high-T_c oxides. *Phys. Rev. B*, 40:7391–7394, Oct 1989.

[31] Steven R. White and D. J. Scalapino. Density matrix renormalization group study of the striped phase in the 2d t-j model. *Phys. Rev. Lett.*, 80:1272–1275, Feb 1998.

[32] D.J. Scalapino and S.R. White. Stripe structures in the t–t'-j model. *Physica C: Superconductivity*, 481(0):146 – 152, 2012.

[33] Hiroyuki Yamase and Hiroshi Kohno. Instability toward formation of quasi-one-dimensional fermi surface in two-dimensional t-j model. *J. Phys. Soc. Jpn.*, 69(7):2151–2157, 2000.

[34] Hae-Young Kee, Eugene H. Kim, and Chung-Hou Chung. Signatures of an electronic nematic phase at the isotropic-nematic phase transition. *Phys. Rev. B*, 68(24):245109, Dec 2003.

[35] W. Metzner, D. Rohe, and S. Andergassen. Soft fermi surfaces and breakdown of fermi-liquid behavior. *Phys. Rev. Lett.*, 91(6):066402, Aug 2003.

[36] Hiroyuki Yamase, Vadim Oganesyan, and Walter Metzner. Mean-field theory for symmetry-breaking fermi surface deformations on a square lattice. *Phys. Rev. B*, 72(3):035114, Jul 2005.

[37] Christoph J. Halboth and Walter Metzner. d-wave superconductivity and Pomeranchuk instability in the two-dimensional Hubbard model. *Phys. Rev. Lett.*, 85(24):5162–5165, Dec 2000.

[38] Mark H. Fischer and Eun-Ah Kim. Mean-field analysis of intra-unit-cell order in the emery model of the CuO_2 plane. *Phys. Rev. B*, 84:144502, Oct 2011.

[39] G. Seibold, C. Castellani, C. Di Castro, and M. Grilli. Striped phases in the two-dimensional Hubbard model with long-range Coulomb interaction. *Phys. Rev. B*, 58:13506–13509, Nov 1998.

[40] Masanori Ichioka and Kazushige Machida. Electronic structure of stripes in two-dimensional Hubbard model. *Journal of the Physical Society of Japan*, 68(12):4020–4031, 1999.

[41] B. Normand and A. P. Kampf. Lattice anisotropy as the microscopic origin of static stripes in cuprates. *Phys. Rev. B*, 64:024521, Jun 2001.

[42] J. Lorenzana and G. Seibold. Metallic mean-field stripes, incommensurability, and chemical potential in cuprates. *Phys. Rev. Lett.*, 89:136401, Sep 2002.

[43] G. Seibold and J. Lorenzana. Stability of metallic stripes in the one-band extended Hubbard model. *Phys. Rev. B*, 69:134513, Apr 2004.

[44] V.J. Emery and S.A. Kivelson. Frustrated electronic phase separation and high-temperature superconductors. *Physica C: Superconductivity*, 209(4):597 – 621, 1993.

[45] S. A. Trugman. Interaction of holes in a Hubbard antiferromagnet and high-temperature superconductivity. *Phys. Rev. B*, 37:1597–1603, Feb 1988.

[46] V. J. Emery. Theory of high-T_c superconductivity in oxides. *Phys. Rev. Lett.*, 58(26):2794–2797, Jun 1987.

[47] E. Fradkin, S. A. Kivelson, and J. M. Tranquada. Theory of Intertwined Orders in High Temperature Superconductors. arXiv:1407.4480.

[48] K. M. Shen, F. Ronning, W. Meevasana, D. H. Lu, N. J. C. Ingle, F. Baumberger, W. S. Lee, L. L. Miller, Y. Kohsaka, M. Azuma, M. Takano, H. Takagi, and Z.-X. Shen. Angle-resolved photoemission studies of lattice polaron formation in the cuprate $Ca_2CuO_2Cl_2$. *Phys. Rev. B*, 75:075115, Feb 2007.

[49] D. M. Frenkel, R. J. Gooding, B. I. Shraiman, and E. D. Siggia. Ground-state properties of a single oxygen hole in a CuO_2 plane. *Phys. Rev. B*, 41:350–370, Jan 1990.

[50] Bayo Lau, Mona Berciu, and George A. Sawatzky. High-spin polaron in lightly doped CuO_2 planes. *Phys. Rev. Lett.*, 106:036401, Jan 2011.

[51] Steven Kivelson, Eduardo Fradkin, and Theodore Geballe. Quasi-one-dimensional dynamics and nematic phases in the two-dimensional Emery model. *Physical Review B*, 69(14):1–7, April 2004.

[52] S. M. Hayden, G. Aeppli, R. Osborn, A. D. Taylor, T. G. Perring, S-W. Cheong, and Z. Fisk. High-energy spin waves in La_2CuO_4. *Phys. Rev. Lett.*, 67:3622–3625, Dec 1991.

[53] A. Nazarenko, K. J. E. Vos, S. Haas, E. Dagotto, and R. J. Gooding. Photoemission spectra of $Sr_2CuO_2Cl_2$: A theoretical analysis. *Phys. Rev. B*, 51:8676–8679, Apr 1995.

[54] Oleg A. Starykh, Oziel F. de Alcantara Bonfim, and George F. Reiter. Self-consistent born approximation for the hole motion in the three-band model: A comparison with photoemission experiments. *Phys. Rev. B*, 52:12534–12537, Nov 1995.

[55] Matthias Vojta. Lattice symmetry breaking in cuprate superconductors: stripes, nematics, and superconductivity. *Advances in Physics*, 58(6):699–820, November 2009.

[56] S A Kivelson, I P Bindloss, E Fradkin, V Oganesyan, J. M. Tranquada, A. Kapitulnik, and C. Howald. How to detect fluctuating stripes in the high-temperature superconductors. *Reviews of Modern Physics*, 75(4):1201–1241, October 2003.

[57] Boris I. Shraiman and Eric D. Siggia. Mobile vacancy in a quantum antiferromagnet: Effective hamiltonian. *Phys. Rev. B*, 42:2485–2500, Aug 1990.

[58] M. Hücker, G. D. Gu, and J. M. Tranquada. Spin susceptibility of underdoped cuprate superconductors: Insights from a stripe-ordered crystal. *Phys. Rev. B*, 78:214507, Dec 2008.

[59] Andreas Lüscher, Grégoire Misguich, Alexander I. Milstein, and Oleg P. Sushkov. Local spin spirals in the néel phase of $La_{2-x}Sr_xCuO_4$. *Phys. Rev. B*, 73:085122, Feb 2006.

[60] A. Mulder, R. Ganesh, L. Capriotti, and A. Paramekanti. Spiral order by disorder and lattice nematic order in a frustrated Heisenberg antiferromagnet on the honeycomb lattice. *Phys. Rev. B*, 81:214419, Jun 2010.

[61] V. J. Emery, S. A. Kivelson, and H. Q. Lin. Phase separation in the t-j model. *Phys. Rev. Lett.*, 64:475–478, Jan 1990.

[62] A Mesaros, K Fujita, H Eisaki, S Uchida, J C Davis, S Sachdev, J Zaanen, M J Lawler, and Eun-Ah Kim. Topological defects coupling smectic modulations to intra-unit-cell nematicity in cuprates. *Science (New York, N.Y.)*, 333(6041):426–30, July 2011.

[63] Christopher L. Henley. Ordering due to disorder in a frustrated vector antiferromagnet. *Phys. Rev. Lett.*, 62:2056–2059, Apr 1989.

[64] Andrea Di Ciolo, Juan Carrasquilla, Federico Becca, Marcos Rigol, and Victor Galitski. Spiral antiferromagnets beyond the spin-wave approximation: Frustrated xy and Heisenberg models on the honeycomb lattice. *Phys. Rev. B*, 89:094413, Mar 2014.

[65] M. Fujita, H. Goka, K. Yamada, J. M. Tranquada, and L. P. Regnault. Stripe order, depinning, and fluctuations in $La_{1.875}Ba_{0.125}CuO_4$ and $La_{1.875}Ba_{0.075}Sr_{0.050}CuO_4$. *Phys. Rev. B*, 70:104517, Sep 2004.

[66] N. Ichikawa, S. Uchida, J. M. Tranquada, T. Niemöller, P. M. Gehring, S.-H. Lee, and J. R. Schneider. Local magnetic order vs superconductivity in a layered cuprate. *Phys. Rev. Lett.*, 85:1738–1741, Aug 2000.

[67] Kai Sun, Michael J Lawler, and Eun-ah Kim. Spin-Charge Interplay in Electronic Liquid Crystals: Fluctuating Spin Stripe Driven by Charge Nematic Ordering. *Physical Review Letters*, 104(10):1–4, March 2010.

[68] R. M. Fernandes, A. V. Chubukov, J. Knolle, I. Eremin, and J. Schmalian. Preemptive nematic order, pseudogap, and orbital order in the iron pnictides. *Phys. Rev. B*, 85:024534, Jan 2012.

[69] Oron Zachar, S. A. Kivelson, and V. J. Emery. Landau theory of stripe phases in cuprates and nickelates. *Phys. Rev. B*, 57:1422–1426, Jan 1998.

[70] K. Fujita, M. H. Hamidian, S. D. Edkins, C. K. Kim, Y. Kohsaka, M. Azuma, M. Takano, H. Takagi, H. Eisaki, S. Uchida, A. Allais, M. J. Lawler, E.-A. Kim, S. Sachdev, and J. C. Séamus Davis. Intra-unit-cell Nematic Density Wave: Unified Broken-Symmetry of the Cuprate Pseudogap State. PNAS 111 E302632.

[71] K. B. Efetov, H. Meier, and C. Pepin. Pseudogap state near a quantum critical point. *Nat Phys*, 9(7):442–446, 07 2013.

[72] Tobias Holder and Walter Metzner. Incommensurate nematic fluctuations in two-dimensional metals. *Phys. Rev. B*, 85:165130, Apr 2012.

[73] Christoph Husemann and Walter Metzner. Incommensurate nematic fluctuations in the two-dimensional Hubbard model. *Phys. Rev. B*, 86:085113, Aug 2012.

[74] W. A. Atkinson, A. P. Kampf, and S. Bulut. Charge Order in the Pseudogap Phase of Cuprate Superconductors. arXiv:1404.1335.

[75] G. Aeppli, T. E. Mason, S. M. Hayden, H. A. Mook, and J. Kulda. Nearly singular magnetic fluctuations in the normal state of a high-tc cuprate superconductor. *Science*, 278(5342):1432–1435, 1997.

[76] M. Enoki, M. Fujita, T. Nishizaki, S. Iikubo, D. K. Singh, S. Chang, J. M. Tranquada, and K. Yamada. Spin-stripe density varies linearly with the hole content in single-layer $Bi_{2+x}Sr_{2-x}CuO_{6+y}$ cuprate superconductors. *Phys. Rev. Lett.*, 110:017004, Jan 2013.

[77] S. Blanco-Canosa, A. Frano, E. Schierle, J. Porras, T. Loew, M. Minola, M. Bluschke, E. Weschke, B. Keimer, and M. Le Tacon. Resonant X-ray Scattering Study of Charge Density Wave Correlations in YBa$_2$Cu$_3$O$_{6+x}$. *ArXiv e-prints*, June 2014.

Appendix A. Diagonalization of the hole Hamiltonian

Appendix A.1. Antiferromagnetic configuration

For the long-range Néel antiferromagnetic order, *i.e.*, $S_i^z = \frac{1}{2}(-1)^{i_x+i_y}$, the Hamiltonian equation (2) becomes

$$\mathcal{H} = \frac{t_a - t_b}{2} \sum_{\langle IiI'\rangle,s} \hat{p}^\dagger_{Is}\hat{p}_{I's} + \frac{t_a + t_b}{2} \sum_{\langle IiI'\rangle,s} s(-1)^{i_x+i_y}(\hat{p}^\dagger_{Is}\hat{p}_{I's}) - t_{pp} \sum_{\langle II'\rangle,s} \hat{p}^\dagger_{Is}\hat{p}_{I's} - \frac{NJ_1}{2}, \tag{A.1}$$

where the exchange term between O and Cu atoms is zero due to the zero total spin component in the z direction. Opposite spin components are decoupled, therefore the hole part of the Hamiltonian can be written as $\mathcal{H} = \sum'_{\mathbf{k},s} \psi^\dagger_{\mathbf{k}s}\mathcal{H}_{\mathbf{k}s}\psi_{\mathbf{k}s}$ with $\psi^\dagger_{\mathbf{k}s} = (p_{x\mathbf{k}s}, p_{y\mathbf{k}s}, p_{x\mathbf{k}+\mathbf{Q}s}, p_{y\mathbf{k}+\mathbf{Q}s})^\dagger$, $\mathbf{Q} = (\pi, \pi)$. Note that the sum $\sum'_{\mathbf{k},s}$ here only runs over the folded Brillouin zone. The momentum part is given by

$$\mathcal{H}_{\mathbf{k}s} = \begin{pmatrix} \mathcal{H}_1(\mathbf{k}) & s\mathcal{H}_2(\mathbf{k}) \\ s\mathcal{H}_2^\dagger(\mathbf{k}) & \mathcal{H}_1(\mathbf{k}+\mathbf{Q}) \end{pmatrix}, \tag{A.2}$$

where

$$\mathcal{H}_1(\mathbf{k}) = \begin{pmatrix} (t_a - t_b)\cos k_x & 2(t_a - t_b - 2t_{pp})\cos\frac{k_x}{2}\cos\frac{k_y}{2} \\ 2(t_a - t_b - 2t_{pp})\cos\frac{k_x}{2}\cos\frac{k_y}{2} & (t_a - t_b)\cos k_y \end{pmatrix}, \tag{A.3}$$

$$\mathcal{H}_2(\mathbf{k}) = (t_a + t_b) \begin{pmatrix} i \sin k_x & 2i \cos \frac{k_x}{2} \sin \frac{k_y}{2} \\ 2i \sin \frac{k_x}{2} \cos \frac{k_y}{2} & i \sin k_y \end{pmatrix}. \tag{A.4}$$

Diagonalization of the matrices leads to the band structure for spin up and down holes, which are degenerate.

Appendix A.2. Spiral configurations

The spiral spin pattern is given by $\vec{S}_i = S(\cos \mathbf{Q} \cdot \mathbf{r}_i, \sin \mathbf{Q} \cdot \mathbf{r}_i, 0)$ and the Hamiltonian equation (2) can again be written in closed form in momentum space as $\mathcal{H} = \sum_{\mathbf{k}} \psi^\dagger_{\mathbf{k}} \mathcal{H}(\mathbf{k}) \psi_{\mathbf{k}}$, now with $\psi^\dagger_{\mathbf{k}} = (p_{x,\mathbf{k},-\mathbf{Q}\uparrow}, p_{y,\mathbf{k}-\mathbf{Q}\uparrow}, p_{x,\mathbf{k}\downarrow}, p_{y,\mathbf{k}\downarrow})^\dagger$, where

$$\mathcal{H}(\mathbf{k}) = \begin{pmatrix} \mathcal{H}_1(\mathbf{k}-\mathbf{Q}) & \mathcal{H}_2(\mathbf{k},\mathbf{Q}) \\ \mathcal{H}_2^{\mathrm{T}}(\mathbf{k},\mathbf{Q}) & \mathcal{H}_1(\mathbf{k}) \end{pmatrix} \tag{A.5}$$

with $\mathcal{H}_1(\mathbf{k})$ given in equation (A.3) and

$$\mathcal{H}_2(\mathbf{k},\mathbf{Q}) = 2S(t_a+t_b) \begin{pmatrix} \cos(k_x - \frac{Q_x}{2}) + J_2 \cos \frac{Q_x}{2} & 2 \cos \frac{k_y}{2} \cos(\frac{k_x}{2} - \frac{Q_x}{2}) \\ 2 \cos \frac{k_x}{2} \cos(\frac{k_y}{2} - \frac{Q_y}{2}) & \cos(k_y - \frac{Q_y}{2}) + J_2 \cos \frac{Q_y}{2} \end{pmatrix} \tag{A.6}$$

Depending on the direction of spiral propagation we consider a diagonal spiral with $\mathbf{Q} = (\pi - \delta, \pi - \delta)$, a parallel spiral with respect to FM arrangement with $\mathbf{Q} = (\pi - \delta, 0)$, and a parallel spiral with respect to AFM arrangement with $\mathbf{Q} = (\pi - \delta, \pi)$. Figure 2 summarizes the spiral patterns we considered.